

Article

High-Temperature Oxidation Behaviors of TA15 Titanium Alloy after Mechanical Grinding and Laser Cleaning

Zhi-Chao Li ^{1,2}, Jie Xu ^{1,2,*}, Dong-He Zhang ^{1,2}, Zhen-Hai Xu ^{1,2}, Shi-Rui Yang ³, De-Bin Shan ^{1,2} and Bin Guo ^{1,2,*}

- ¹ Key Laboratory of Micro-Systems and Micro-Structures Manufacturing of Ministry of Education, Harbin Institute of Technology, Harbin 150080, China; zhichaoli1234@163.com (Z.-C.L.); zhangdonghehit@163.com (D.-H.Z.); xzhenhai@163.com (Z.-H.X.); shandb@hit.edu.cn (D.-B.S.)
- ² School of Materials Science and Engineering, Harbin Institute of Technology, Shenzhen 518055, China
- ³ Beijing Power Machinery Research Institute, Beijing 100074, China; fallsaint@163.com
- * Correspondence: xjhit@hit.edu.cn (J.X.); bguo@hit.edu.cn (B.G.); Tel.: +86-0451-86403958 (J.X.); +86-0451-86418183 (B.G.)

Abstract: This paper presents the results of a study on the high-temperature oxidation characteristics after mechanical and laser removal of TA15 titanium alloy oxide film. The morphology, components, and roughness of the surface were characterized by scanning electron microscope (SEM), X-ray diffraction (XRD), X-ray photoelectron spectroscopy (XPS) and laser confocal microscope (OM). The oxide film can be effectively removed with mechanical grinding and laser cleaning, and the oxide film after mechanical grinding is thicker and looser than that of after laser cleaning. The oxide film is principally composed of TiO₂, Ti₂O₃ and TiO. Besides, there is a small amount of aluminum oxide on the surface. The surface after mechanical grinding was rougher than that of after laser cleaning. Thus, this work indicates that laser can not only clean the oxide film completely, but also strengthen the surface, which is a promising way to favor the widespread application of laser cleaning technology.

Keywords: high-temperature oxidation; mechanical grinding; laser cleaning; surface roughness; titanium alloy



Citation: Li, Z.-C.; Xu, J.; Zhang, D.-H.; Xu, Z.-H.; Yang, S.-R.; Shan, D.-B.; Guo, B. High-Temperature Oxidation Behaviors of TA15 Titanium Alloy after Mechanical Grinding and Laser Cleaning. *Coatings* **2021**, *11*, 1090. <https://doi.org/10.3390/coatings11091090>

Academic Editor: Pier Luigi Bonora

Received: 10 August 2021
Accepted: 7 September 2021
Published: 9 September 2021

Publisher's Note: MDPI stays neutral with regard to jurisdictional claims in published maps and institutional affiliations.



Copyright: © 2021 by the authors. Licensee MDPI, Basel, Switzerland. This article is an open access article distributed under the terms and conditions of the Creative Commons Attribution (CC BY) license (<https://creativecommons.org/licenses/by/4.0/>).

1. Introduction

Titanium, a very reactive metal, is easy to form oxide film with, which has characteristics of being thin, stable, adherent and compact, and is often applied in aerospace, chemical, medical and electrochemical industries [1–4]. However, the oxide film on titanium alloy will be formed during long-term storage and high-temperature forming for strong oxidation diffusion ability [5]. Joanna Małecka [6] researched the kinetics of oxidation and the oxide scale morphologies on Ti₂AlNb at 700 and 800 °C in air, and the oxide film is composed of TiO₂ and Al₂O₃. R. Mythili [7] studied the corrosion mechanism of the Ti–5%Ta–1.8%Nb alloy passive oxide film, and the component of passive oxide film is anatase-TiO₂ and a small amount of Nb₂O₅ and Ta₂O₅. Kai Ma [8] obtained the ideal cutting temperature range by studying the oxidation mechanism of biomedical titanium alloy. I. Jouanny [9] found that the anatase-TiO₂ film could be the best candidate as a titanium oxide intermediate layer between hydroxyapatite and titanium alloy in the field of biomedical implants. Y. Tanaka [10] searched that the oxide film of Ti–29Nb–13Ta–4.6Zr was a Ti, Nb, Ta and Zr very thin composite oxide. Maja Voncina [11] analyzed the oxidation resistance of titanium alloys. The Al and V can improve oxidation resistance. Soon Yong Park [12] proved Al, Nb and Si to increase the oxidation resistance of Ti–44Al–6Nb–2Cr–0.3Si–0.1C alloy, and Nb, Cr and Si have tended to segregate the oxide scale-matrix interface. Dongjun Wang [13] investigated the oxidation behaviors of the TA15 titanium alloy and TiBw/TA15 composite in the temperature range of 873–1073 K, and TiBw/TA15 composite exhibited a higher oxidation resistance than TA15. It is of great significance to study the oxidation properties of titanium alloy for its subsequent application.

Laser cleaning, which was often used to remove oxide film, paint, rust and microorganism, is a new green and efficient cleaning technology. Aniruddha Kumar [14] applied pulsed fiber laser to clean the Ti–3Al–2.5V tubes for welding. The tube surface microhardness was improved after laser cleaning. Yao Lu [15] found that the surface roughness and corrosion resistance of the AH36 steel were, respectively, reduced and increased after laser cleaning. Ze Tian [16,17] obtained superhydrophobicity and an antibacterial surface with laser cleaning micro-biofouling from the aluminum alloy. Tianyi Shi [18] applied a 120 W mopa pulsed fiber laser to remove the oxide film on aluminum alloy, and the tensile and bending properties were improved. Qiyu Gao [19] analyzed the adhesive bonding tensile properties of residual resin and surface energy by controlling the ultraviolet (UV) laser cleaning the carbon fiber resin matrix reinforced polymer (CFRP). Laser cleaning is beneficial to improve the bonding properties of CFRP sheets. Buxiang Zheng [20] successfully used ultra-fast laser pulses to produce the self-cleaning property of a micro/nanostructured surface. Shusen Zhuang [21] studied the corrosion properties of bare carbon steel plates after laser cleaning. The corrosion resistance of carbon steel plates was improved for denser iron oxide formed when higher laser power density was irradiated. Bowen Liu [22] studied how the wear resistance of material was strengthened by grain refinement after laser cleaning. The surface after laser cleaning often has high wear resistance, hydrophobicity and hardness. Besides, surface roughness after laser cleaning played an important role in the machinability and corrosion resistance of materials. Roughness is usually represented by average surface roughness (Ra), the average height of element of roughness profile (Rc) and the maximum height of roughness profile (Rz) [23]. The height change of the surface profile has a direct impact on the change of surface roughness [24]. However, there is no detailed study on the oxidation resistance of the material surface by laser cleaning. The oxidation behavior between mechanical grinding and laser cleaning was also not reported.

In our paper, we first applied silicon carbide (SiC) paper and laser to remove natural oxide films on TA15 titanium alloy. Then, the samples, after removing oxide film, were heated at 800 °C in air for different times. Finally, the composition and morphology of oxide film was analyzed with a scanning electron microscope (FE-SEM), X-ray diffraction (XRD), X-ray photoelectron spectroscopy (XPS) and a laser scanning confocal microscope (OM). Then, the surface oxidation behavior of titanium alloy after mechanical grinding and laser cleaning was analyzed.

2. Materials and Methods

The material used in this experiment is TA15 titanium alloy (Ti-89.5 wt.%, Al-6.5 wt.%, Mo-1 wt.%, V-1 wt.%, Zr-2 wt.%) sheets. The TA15 sample, with initial oxide film after long-term storage, was trimmed into fifty-six pieces samples (20 mm × 20 mm × 2 mm). The twenty-eight samples were abraded with silicon carbide (SiC) paper, successive grades from 200 to 2000, grit to remove oxide film (mechanical grinding). The other samples were cleaned, the oxide film from TA15 titanium alloy by nanosecond pulse laser. The laser cleaning system used an IPG ytterbium pulsed laser (IPG Photonics, Oxford, Ma, USA) as the laser source, with a 100 ns pulse duration, 1064 nm wavelength, 500 W power and 20 kHz repetition rate. Then, all samples were ultrasonically cleaned in ethanol solution, degreased in alkaline, rinsed in deionized water and retained after vacuum drying. Finally, the samples were continuously heated and oxidized in air at 800 °C isothermal conditions tubular furnace. The four samples were taken out and tested at oxidation time of 0.5, 1, 2, 4, 6, 8 and 10 h after mechanical grinding and laser cleaning, respectively. The experimental scheme is shown in Figure 1.

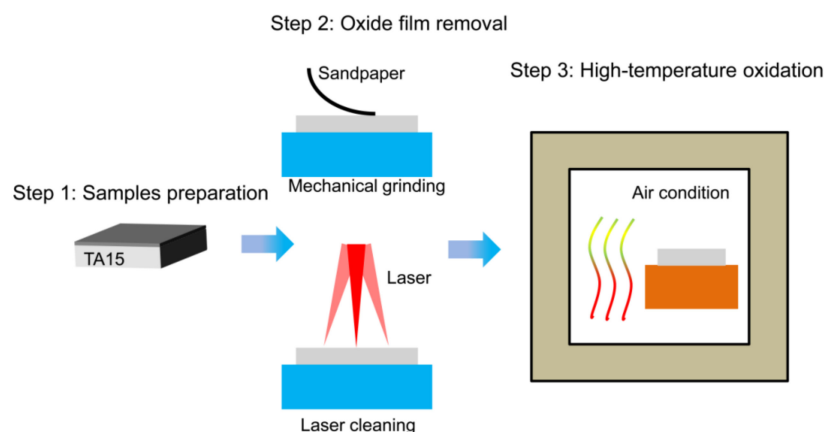


Figure 1. Schematic diagram of experimental scheme.

The surface morphology and oxide film thickness of samples were observed by means of laser scanning confocal microscope (OM, Olympus, Tokyo, Japan) and scanning electron microscope (FE-SEM, Quanta 200FEG, FEI, Hillsboro, OR, USA). The phase composition and changes of the surface in the elemental contents were measured by X-ray diffraction (XRD, Empyrean, Panalytical, Almolo, Holland) and X-ray photoelectron spectroscopy (XPS, ESCALAB 250Xi, ThermoFisher, Waltham, MA, USA). The high-temperature oxidation behavior of TA15 titanium alloy was studied by comparing the changes of oxide film composition and morphology after oxidation. Vickers microhardness was measured by digital microhardness tester (HVS-1000A, Laizhou Huayin Instrument Co., Ltd, Laizhou, China).

3. Results

3.1. Surface Morphology Analyses

Figure 2a displays surface morphology of original samples. There are lots of particles and pits on the surface, and the subsequent forming of materials will be unsatisfactory. Figure 2b,c show the surface topography of TA15 titanium alloy after original oxide film was removed by mechanical and laser treatment, respectively. The scratches were formed on the TA15 titanium alloy surface after silicon carbide (SiC) paper removal of the original oxide film. However, the surface is smooth without damage material for laser cleaning.

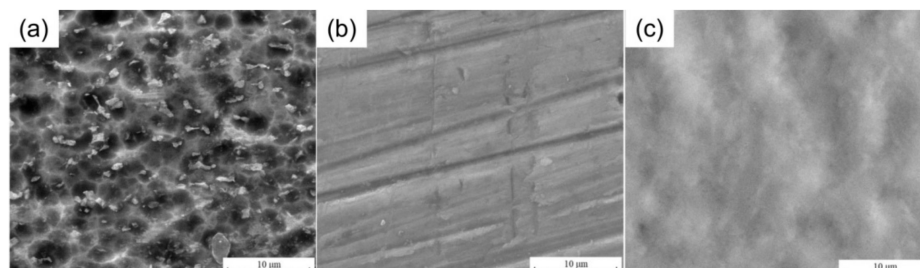


Figure 2. Surface morphology of TA15 titanium alloy: (a) Original sample (b) mechanical grinding, (c) laser cleaning.

The surface morphologies of TA15 titanium alloy sheets after high-temperature oxidation that have been, respectively, treated with mechanical and laser to remove original oxide film are shown in Figure 3. For mechanical grinding, the lamellar structure is formed after oxidation for 0.5 h heating at 800 °C, then continues to grow by increasing oxidation time. The granular structure will appear on the surface as the oxidation time increases to 2 h. The surface oxide film will produce acicular structure at 6 h, so the oxide film porosity was increased. The surface acicular and laminar structure continues to grow, then forms a porous structure in Figure 3e. However, the oxide film continues to grow

and the porosity decreases in Figure 3f. Compared with mechanical grinding, uniformly distributed particles formed on the surface after laser cleaning for 0.5 h at 800 °C, and there is no acicular structure during the growth of oxide film. The material surface does not easily form a lamellar structure in a short time. With the increase of heating time, the surface oxide particles increase continuously, and formed lamellar structure or large particle structure in Figure 3j,l.

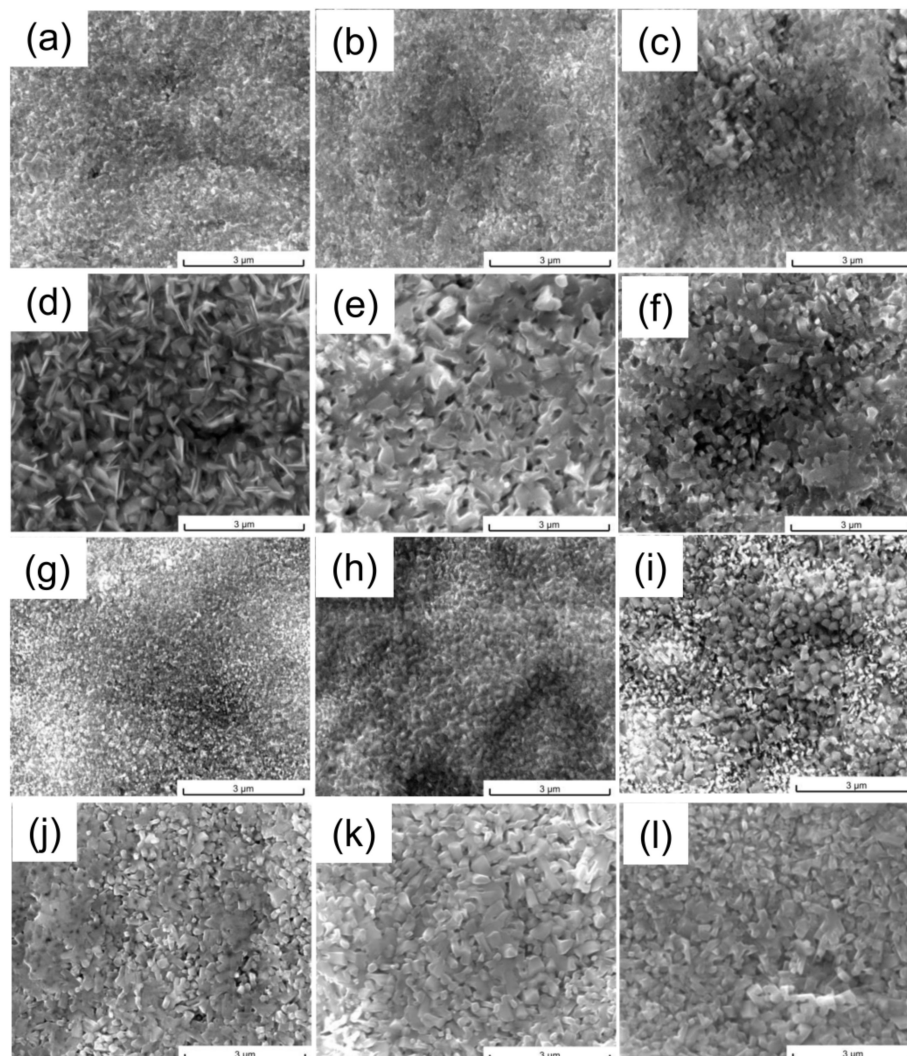


Figure 3. Microscopic SEM images of the removal oxide film surfaces with different heating times: (a–f) mechanical grinding, (a) 0.5 h, (b) 1 h, (c) 2 h, (d) 4 h, (e) 6 h and (f) 8 h; (g–l) laser cleaning, (g) 0.5 h, (h) 1 h, (i) 2 h, (j) 4 h, (k) 6 h and (l) 8 h.

3.2. Section Analyses

Figure 4 shows the cross-section morphology of the oxide film with different removal methods. With the increase of oxidation time, the thickness of the oxide film was increased for the strong oxygen diffusion ability at a high temperature. The upper surface of oxide film is fluffy at 2 and 4 h for mechanical removal of the original oxide film in Figure 4c,d. The high-temperature oxide film was formed on the surface, and the texture is more uniform, but the oxide film will become slightly loose with the time increase. The high-temperature oxide film was more uniform after laser cleaning. The oxide film was thin at 0.5 h. Figure 5 shows the oxide film thickness with different heat treatment time. After laser cleaning, the thickness of the high-temperature oxidation film is only about 0.5 μm in 0.5 h, and the thickness is about 1 μm after mechanical removal of the oxide film. Besides, the diffusion depth of the oxygen

will be further increased with long high-temperature time, and the thickness of the oxide film is increasing. Compared with the mechanically removal oxide film, the surface after laser cleaning can hinder the secondary high-temperature oxidation of titanium alloy, and the oxide film thickness after laser cleaning is always less than that after mechanical removal.

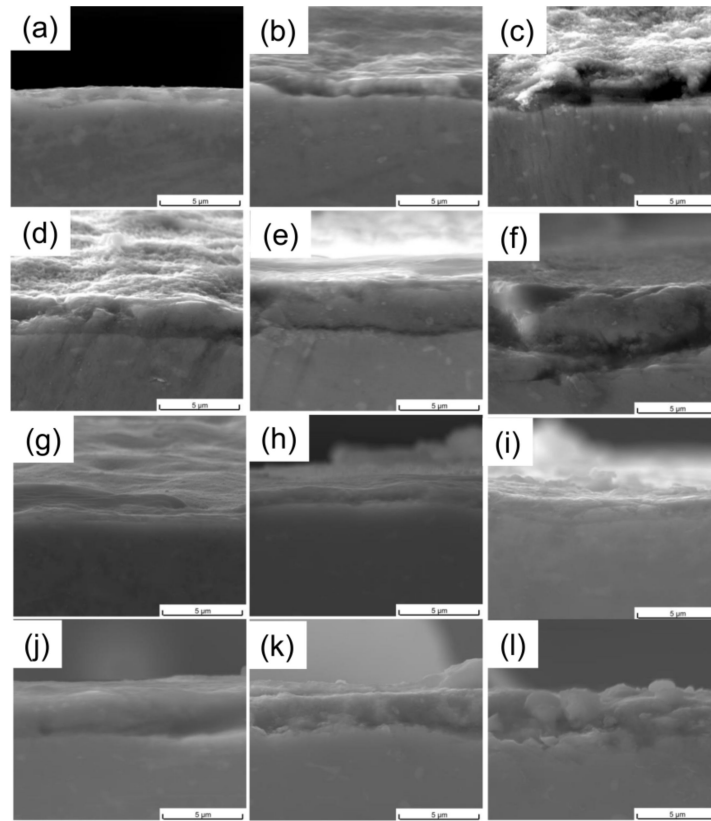


Figure 4. Microscopic SEM images of the removal of the oxide film section with different heating times: (a–f) silicon carbide (SiC) paper, (a) 0.5 h, (b) 1 h, (c) 2 h, (d) 4 h, (e) 6 h and (f) 8 h; (g–l) laser cleaning, (g) 0.5 h, (h) 1 h, (i) 2 h, (j) 4 h, (k) 6 h and (l) 8 h.

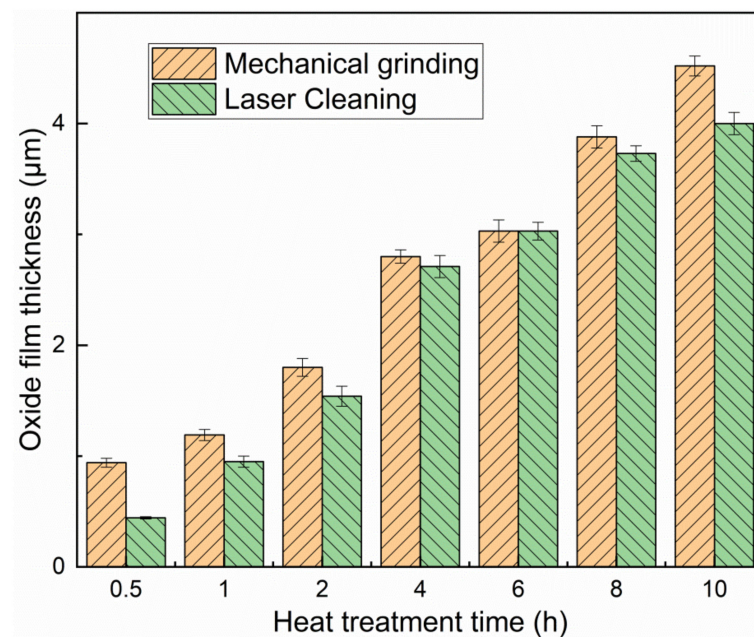


Figure 5. The thickness of the oxide film under different treatment methods and heating times.

In order to study the composition distribution of the high-temperature oxidation sample, the energy spectrum curves are measured from the surface vertical to the substrate. Figure 6 shows energy spectrum curves of oxide film after high-temperature oxidation. The oxide film thickness is comprised as in Figure 5. The main components of the oxide film are Al, Ti and O, and the oxide film consisted of titanium oxides and alumina. Oxygen not only forms oxide film on the surface, but also a small amount of oxygen will also diffuse into the substrate for strong diffusion at a high temperature [6,11,12]. The aluminum content is concentrated on the upper surface for the sample after laser cleaning, which can inhibit the further oxidation of titanium alloy. Therefore, the high-temperature oxide film thickness after mechanical grinding is greater than that after laser cleaning. After laser cleaning, aluminum in titanium alloy will be more easily enriched or form nano scale alumina film under the residual heat of the laser [16], and aluminum is more active than titanium and it is easy to form alumina on the upper surface [13,25]. Therefore, the surface after laser cleaning will inhibit the further oxidation of titanium alloy. With the oxidation time increase, the aluminum content is limited, and the inhibition oxidation effect is weakened, so the oxide film growth rate slightly increases. In addition, there will be small scratches on the TA15 titanium alloy after mechanical cleaning, which will increase the contact area between the material and oxygen, and also further promote the oxidation ability of mechanical removal.

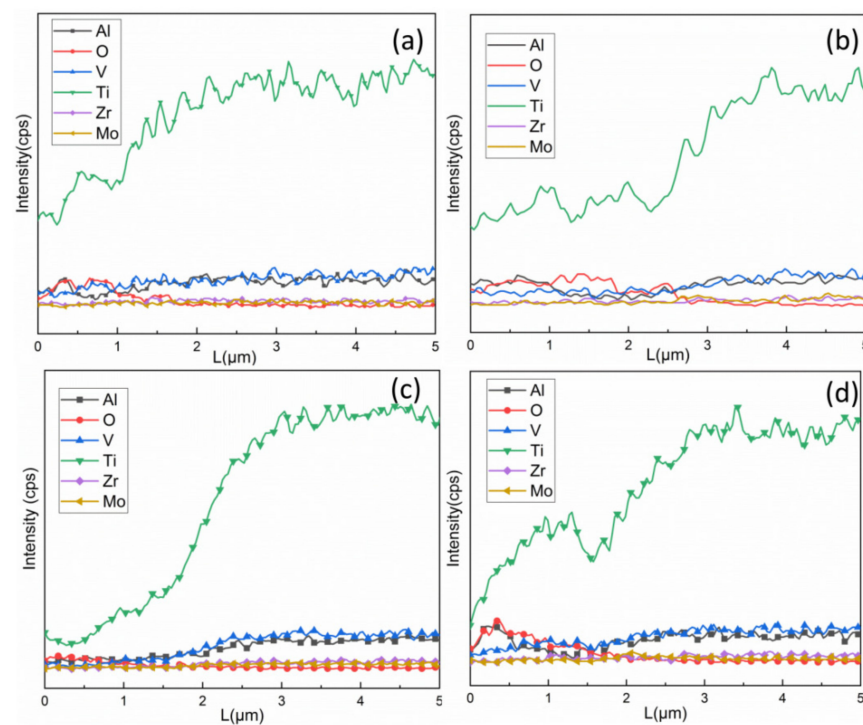


Figure 6. The contents of different elements change with depth at 800 °C: (a) 0.5 h and (b) 2 h after mechanical grinding, (c) 0.5 h and (d) 2 h after laser cleaning.

3.3. XPS Analyses

The XPS survey spectrum of TA15 oxide films was recorded after high-temperature oxidation in air condition (0.5 h), as shown by Figure 7. Results show that the dominant surface elements are O, Ti and Al, which suggests titanium oxides and alumina were formed. The C and N elements identified by XPS may be from the air. The results indicate that the surface formed titanium and aluminum oxide during high-temperature oxidation in air.

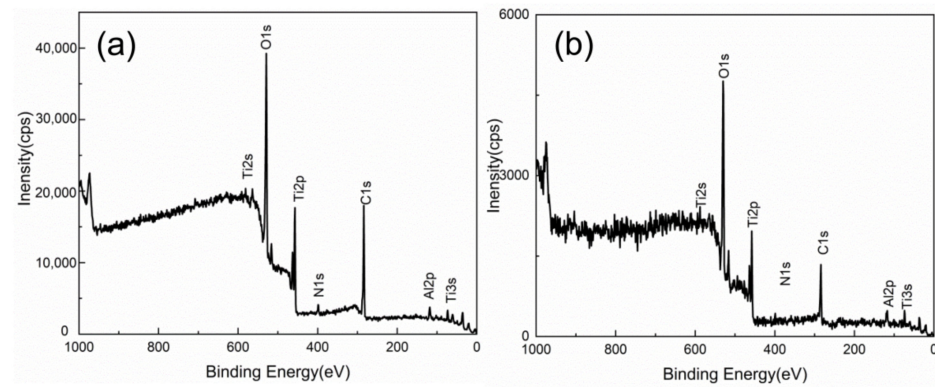


Figure 7. XPS survey spectrum of high-temperature oxide films at 800 °C for 0.5 h: (a) Mechanical grinding, (b) Laser cleaning.

Figure 8 presents Ti 2p XPS spectra of re-oxidation at 0.5, 2 and 10 h after removing oxide film by mechanical grinding and laser cleaning. The Ti 2p spectra displayed three oxidation states of Ti^{4+} (2p_{3/2} peaks at 459.2 ± 0.2 and 2p_{1/2} peaks of at 465.0 ± 0.2), Ti^{3+} (2p_{1/2} peaks at 463.5 ± 0.2) and Ti^{2+} (2p_{1/2} peaks at 461.5 ± 0.2) [26,27]. Oxygen is rapidly diffused into the material at high temperature, then the thicker oxide film can be formed with time increases. The oxide film is mainly composed of Ti^{4+} , a small amount of Ti^{3+} and Ti^{2+} . With the increase of heating time, the content of Ti^{4+} increased significantly. The Ti^{3+} and Ti^{2+} obtained energy at high temperature and further reacted to Ti^{4+} . However, there are always Ti^{4+} , Ti^{3+} and Ti^{2+} in the oxide film.

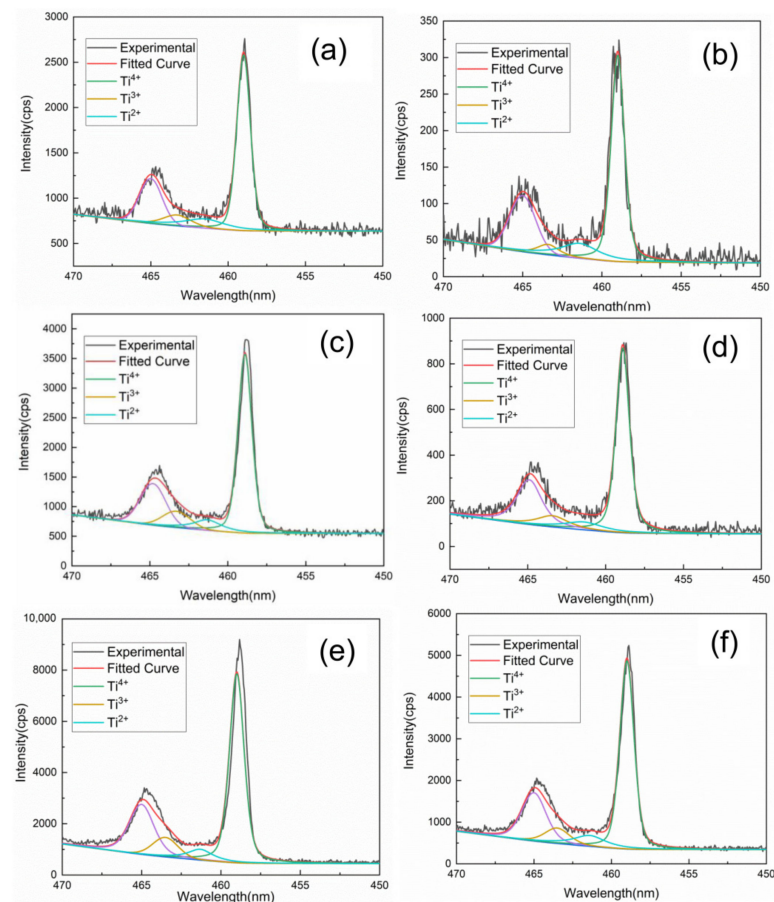


Figure 8. XPS spectrum of Ti 2p at different heating times: (a), (c) and (e) mechanical grinding at 0.5, 2 and 10 h, (b), (d) and (f) laser cleaning at 0.5, 2 and 10 h.

The O 1s photoemission signal could be split in three peaks (Figure 9), the first at the energy of 530.5 eV O^{2+} bonds (Ti–O, Al–O), the second at the energy of 531.7 eV, attributed to OH bonds at (531.8 ± 0.2) eV, and the third at the energy of 532.7 eV, attributed to adsorbed H_2O at (532.6 ± 0.3) eV [28,29]. Oxygen content after mechanical grinding is higher than that after laser cleaning at any heating time. Thus, the surface after laser cleaning can inhibit oxidation of TA15 titanium alloy. The water vapor can be absorbed in the oxidation formation process due to the fluffy oxide film, then the energy spectrum forms a strong water peak at different times.

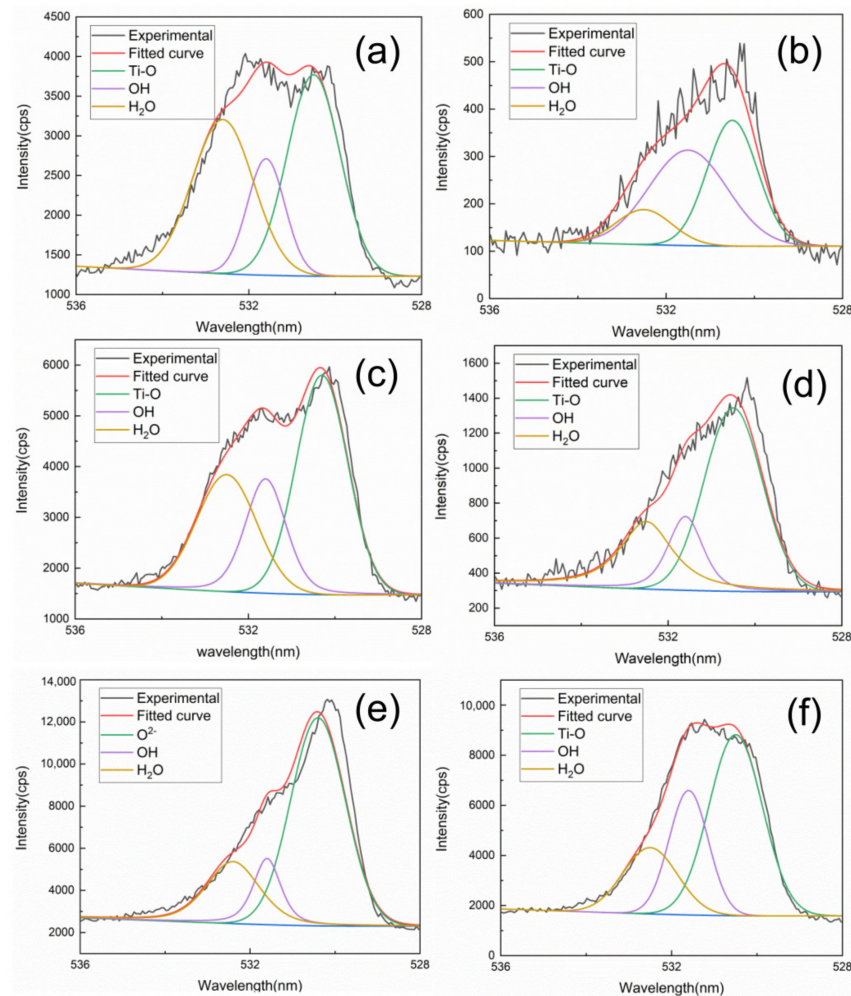


Figure 9. XPS spectrum of O 1s at different heating times: (a), (c) and (e) mechanical grinding at 0.5, 2 and 10 h, (b), (d) and (f) laser cleaning at 0.5, 2 and 10 h.

Figure 10 shows the XPS spectrum of the Al 2p region of oxide film. Aluminum is the second largest alloy composition of TA15 titanium alloy (about 6.5 wt.%), and alumina will be produced in the process of alloy oxidation. Al is stronger than that of titanium in reaction activity, unlike the formation of TiO_2 , Ti_2O_3 and TiO , and has a tendency to form Al_2O_3 . However, the peak intensity of Al 2p is much lower than that of Ti, and laser cleaning is obviously weaker than mechanical grinding. Besides, the energy spectrum peak of Al still exists on the oxide surface after laser cleaning with 0.5–2 h heat treatment time, which indicates that the oxide film may be thinner and the Al element signal in the substrate is collected. Thus, Ti is not only oxidized at high temperature, but alloy elements such as Al will also be oxidized.

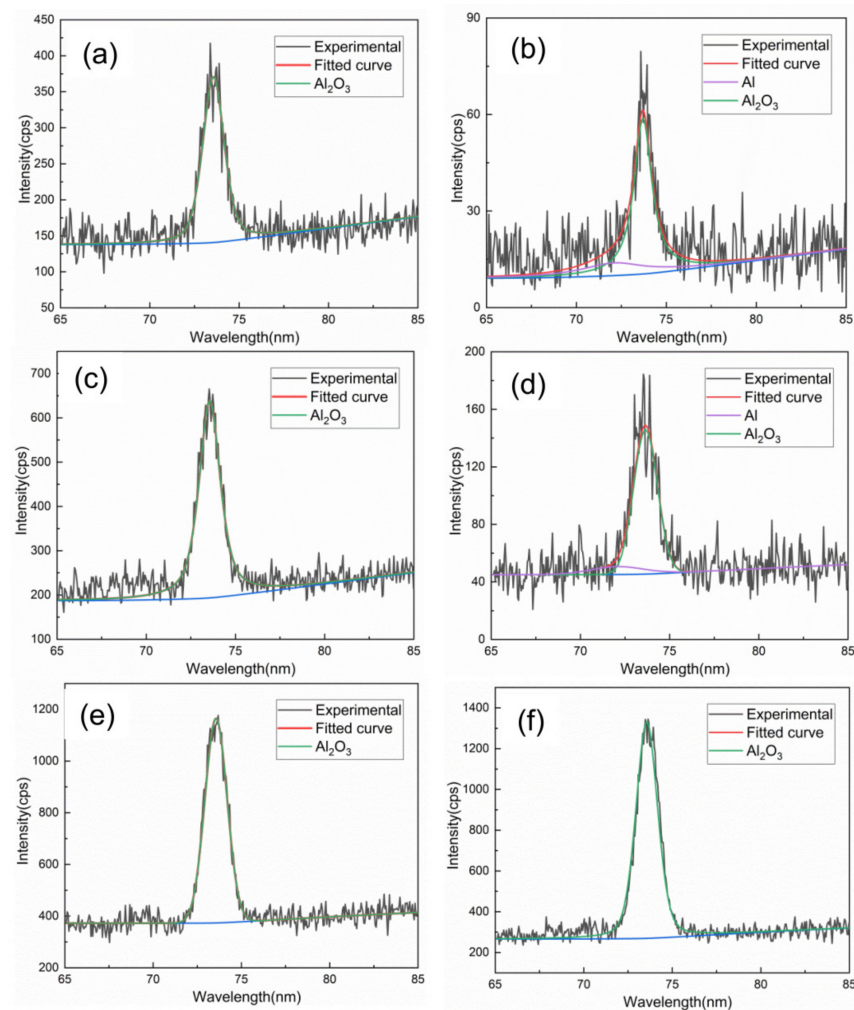


Figure 10. XPS spectrum of Al 2s at different heating times: (a), (c) and (e) mechanical grinding at 0.5, 2 and 10 h, (b), (d) and (f) laser cleaning at 0.5, 2 and 10 h.

3.4. XRD Analyses

The Figure 11 shows the XRD of the sample surface after mechanical grinding and laser cleaning at different heating times. The peaks of anatase-TiO₂, rutile-TiO₂, Ti, Ti₂O₃ and TiO mainly exist on the TA15 titanium alloy surface after removing the original oxide film [13,30]. There is a small amount of aluminum oxide on the surface, and the diffraction peak of aluminum oxide is obviously increased on the sample surface with the increase of heating time, and the anatase phase transformed into rutile titanium dioxide with increasing treatment time. XRD was used to measure the diffraction peak at a certain depth of the surface for semi-qualitative analysis. For the sample after mechanical grinding, the Ti peak decreases rapidly after two hours of heating, while there is still a strong Ti diffraction peak on the sample surface after laser cleaning, indicating that the growth rate of the oxide film after laser cleaning is much lower than that of the mechanical grinding. At the same time, the weak peaks of Ti₂O₃ and TiO still exist on the surface of the mechanical grinding and laser cleaned samples, which are consistent with the XPS analysis results.

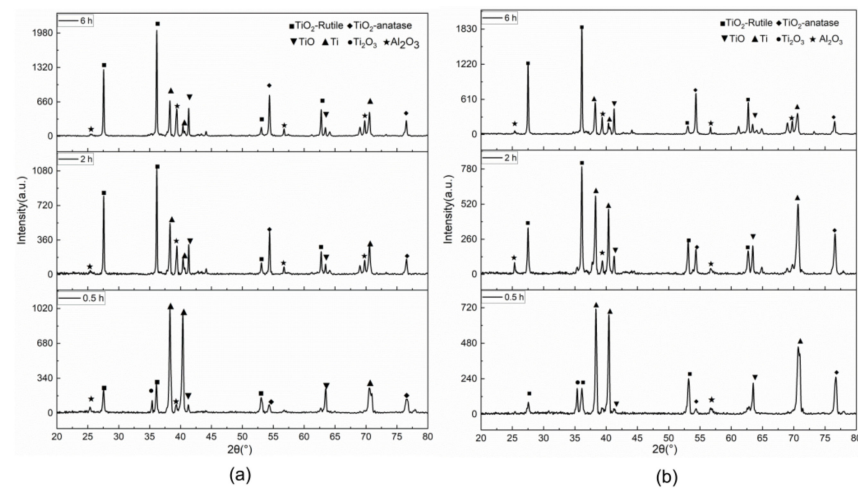


Figure 11. The XPS spectrum at different heating times: (a) mechanical grinding, (b) laser cleaning.

3.5. Roughness Analysis

The surface roughness (R_a) is expressed as an arithmetic mean of the absolute value of contour offset within the specified sampling length. Figures 12 and 13 are surface morphology and roughness of oxide films with heating time. Due to the different speed of oxide film formation on the surface of TA15 after cleaning, there are high and low protrusions on the surface of TA15. The height difference between the wave crest and the wave trough of the material surface section first increases and then decreases with the heating time (Figure 12). The roughness of titanium alloy after oxidation also reflects the new oxide film formation. There will be scratches on the surface after mechanical grinding, so the roughness of mechanical grinding is always higher than that of laser cleaning. After 0.5 h, a small amount of oxide film particles was formed on the surface. The oxide film particles increased slowly and the roughness increased slightly at 1 h. The surface roughness increases to $1.75 \mu\text{m}$ with the increase to 2–4 h. The oxide film particles size on the surface increase when the heating time reaches 6–8 h, and the surface becomes relatively flat. The surface roughness slightly decreases.

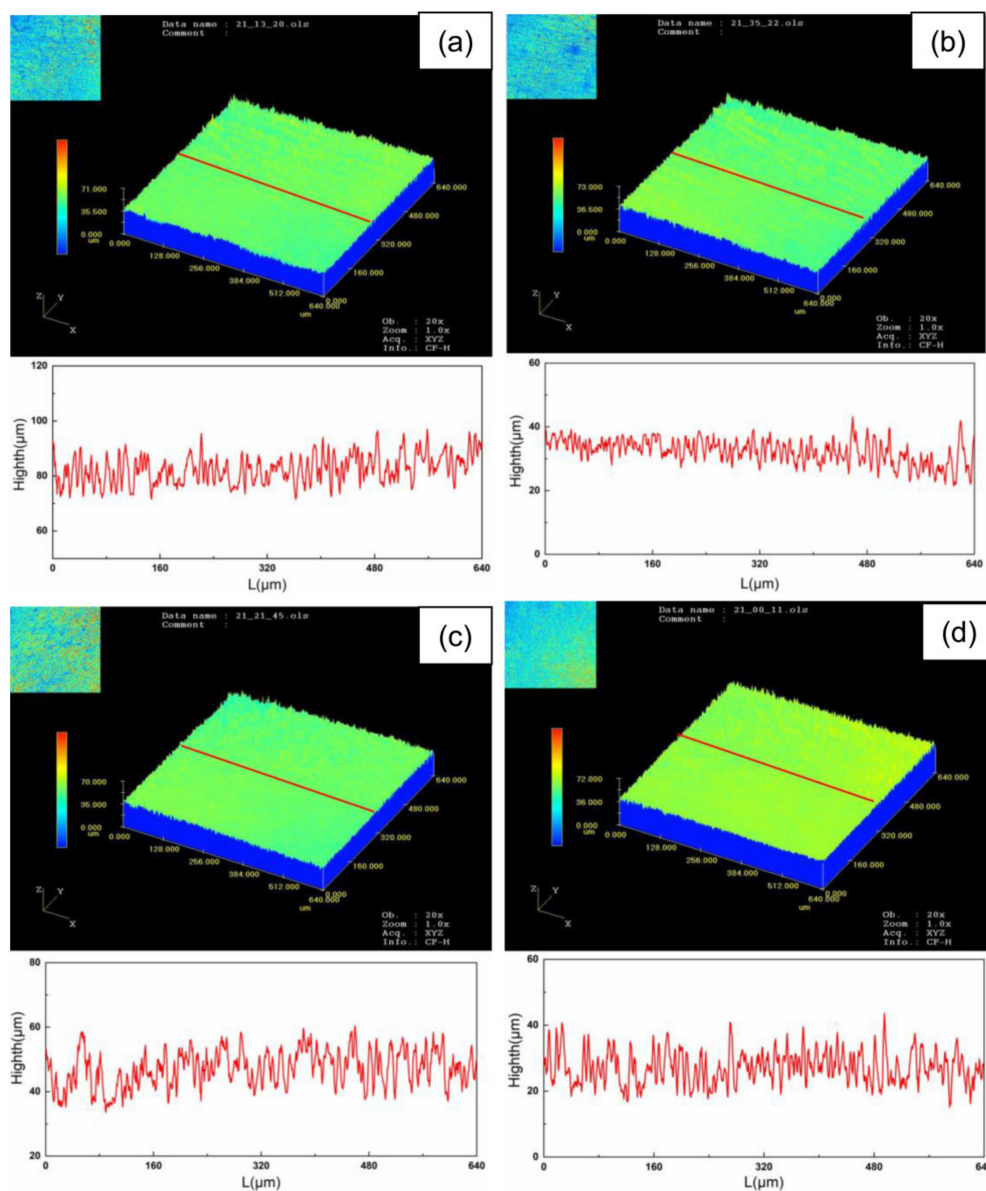


Figure 12. Surface morphology of oxide film at different heating times: (a), (c) mechanical grinding at 0.5 and 2 h, (b), (d) laser cleaning at 0.5 and 2 h.

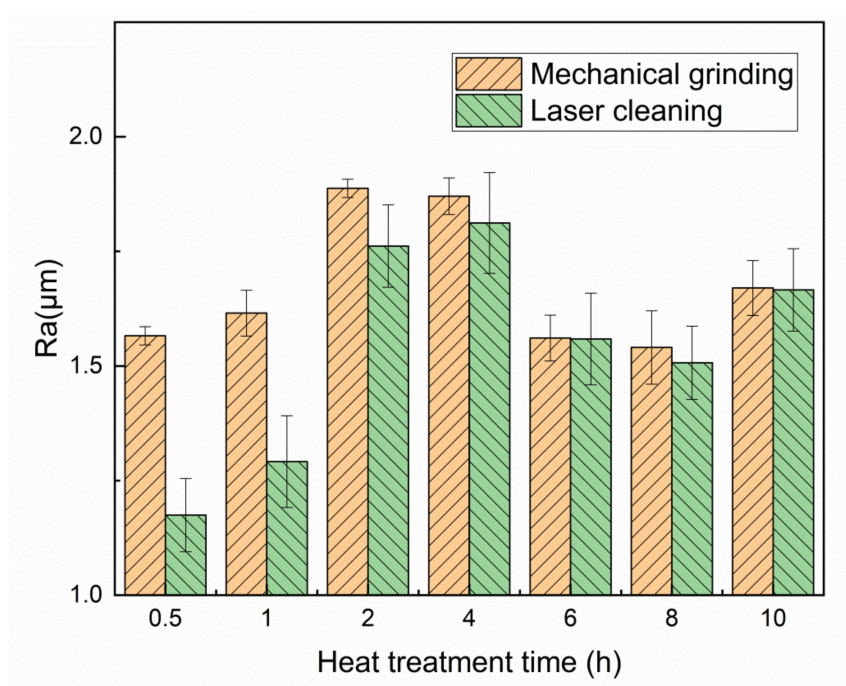


Figure 13. Roughness of surface oxide film at different times with mechanical grinding and laser cleaning.

Figure 14 shows the Vickers hardness data for the mechanical grinding and laser cleaning. Vickers hardness measurement has been carried out by a diamond pyramid indenter under a load of 100 g for 11 s [14]. When the high-temperature treatment time is 0.5 h, the hardness of the laser cleaned surface is 498 HV, which is lower than 556.5 HV after mechanical grinding. The main reason may be that the thickness of oxide film after mechanical grinding is greater than that after laser cleaning. With the increase of high-temperature treatment time, the oxide film hardness was increased.

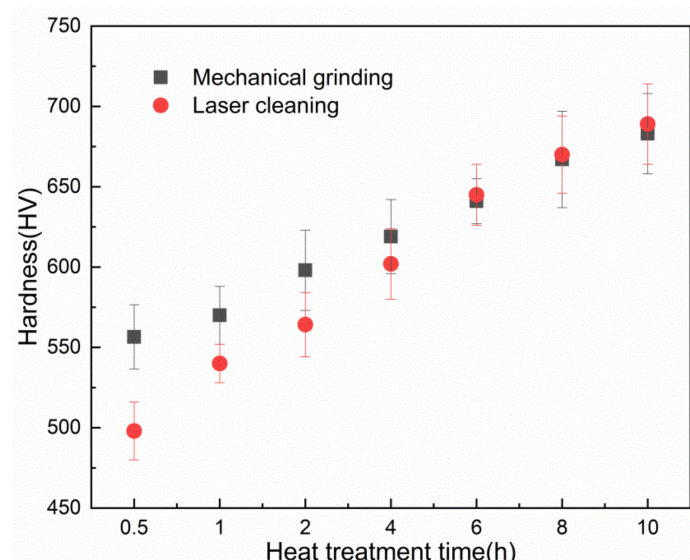


Figure 14. Hardness plot of the laser-cleaned and un-cleaned areas on the tube surface.

4. Conclusions

- (1) Mechanical grinding and laser cleaning can remove titanium alloy oxide film. A small amount of scratches appear on the surface after mechanical grinding. However, the surface is relatively smooth after laser cleaning.

- (2) TA15 titanium alloy is easily oxidized in air at high temperature, and the thickness of oxide film is increased when the high-temperature time increases. Surface roughness increases first and then decreases with time, but hardness increases continuously. Compared with mechanical grinding, TA15 titanium alloy after laser cleaning has high-temperature oxidation resistance.
- (3) The main components of high-temperature oxide film of TA15 titanium alloy after mechanical grinding and laser cleaning are TiO_2 , Ti_2O_3 and TiO , and also contain a small amount of alloy element oxides such as Al_2O_3 . Alumina is mainly concentrated on the surface of the oxide film, which may play an important role in the high-temperature oxidation resistance of titanium alloy.
- (4) Compared with mechanical grinding, laser cleaning technology can provide excellent subsequent processing characteristics, which has great significance for the development of laser cleaning technology.

Author Contributions: Z.-C.L.: conceptualization, data curation, formal analysis, writing—original draft; J.X.: formal analysis, supervision, writing—review & editing; D.-H.Z., Z.-H.X. and D.-B.S.: supervision, writing—review & editing; S.-R.Y.: resources, writing—review & editing; B.G.: funding acquisition, supervision, writing—review & editing. All authors have read and agreed to the published version of the manuscript.

Funding: This work was supported by the National Key R&D Program of China (Program No. 2017YFB1105000), the Guangdong Province Key Area R&D Program (Grant No. 2018B090905003), and the National Natural Science Foundation of China (Grant No. U19A2077).

Institutional Review Board Statement: Not applicable.

Informed Consent Statement: Not applicable.

Data Availability Statement: Data is contained within the article.

Conflicts of Interest: The authors declare no conflict of interest.

References

1. Dimitriu, S.; Dobrescu, M.; Vasilescu, M. Titanium and titanium-based alloys for aerospace. *Metal. Int.* **2009**, *14*, 14–18.
2. Fokin, V.N.; Fokina, E.E.; Tarasov, B.P. Chemical interaction of the Ti94Al6 and Ti91Al9 alloys with ammonia between 150 and 500 °C. *Inorg. Mater.* **2010**, *46*, 1304–1307. [[CrossRef](#)]
3. Koizumi, H.; Takeuchi, Y.; Imai, H.; Kawai, T.; Yoneyama, T. Application of titanium and titanium alloys to fixed dental prostheses. *J. Prosthodont. Res.* **2019**, *63*, 266–270. [[CrossRef](#)]
4. Liu, W.; Ao, S.; Li, Y.; Liu, Z.; Wang, Z.; Luo, Z.; Wang, Z.; Song, R. Jet electrochemical machining of TB6 titanium alloy. *Int. J. Adv. Manuf. Technol.* **2017**, *90*, 2397–2409. [[CrossRef](#)]
5. Li, P.; Li, S.; Li, Y.P.; Li, G.P.; Liu, J.; Wang, J.; Han, P. Effect of titanium addition on the oxidation resistance of Fe–13Cr–5Al–0.3Ti alloy in air between 700 °C–1100 °C. *Mater. Res. Express.* **2018**, *8*, 1–20.
6. Małecka, J. Investigation of the oxidation behavior of orthorhombic Ti_2AlNb Alloy. *J. Mater. Eng. Perform.* **2015**, *24*, 1834–1840. [[CrossRef](#)]
7. Mythili, R.; Saroja, S.; Vijayalakshmi, M. Characterization of passive oxide film on a Ti–5%Ta–1.8%Nb alloy on exposure to severe oxidizing conditions. *Mater. Charact.* **2010**, *61*, 1326–1334. [[CrossRef](#)]
8. Ma, K.; Zhang, R.; Sun, J.; Liu, C. Oxidation mechanism of biomedical titanium alloy surface and experiment. *Int. J. Corros.* **2020**, *2020*, 1–9. [[CrossRef](#)]
9. Jouanny, I.; Labdi, S.; Aubert, P.; Buscema, C.; Maciejak, O.; Berger, M.H.; Guipont, V.; Jeandin, M. Structural and mechanical properties of titanium oxide thin films for biomedical application. *Thin Solid Films* **2010**, *518*, 3212–3217. [[CrossRef](#)]
10. Tanaka, Y.; Nakai, M.; Akahori, T.; Niinomi, M.; Tsutsumi, Y.; Doi, H.; Hanawa, T. Characterization of air-formed surface oxide film on Ti–29Nb–13Ta–4.6Zr alloy surface using XPS and AES. *Corros. Sci.* **2008**, *50*, 2111–2116. [[CrossRef](#)]
11. Vončina, M.; Tisu, R.; Medved, J. Oxidation stability of various Ti-alloys. *J. Therm. Anal. Calorim.* **2017**, *129*, 117–122. [[CrossRef](#)]
12. Park, S.Y.; Seo, D.Y.; Kim, S.W.; Kim, S.E.; Hong, J.K.; Jung, S.B.; Bak, S.H.; Lee, D.B. High-temperature oxidation of Ti–44Al–6Nb–2Cr–0.3Si–0.1C Alloy. *Sci. Adv. Mater.* **2016**, *8*, 2264–2268. [[CrossRef](#)]
13. Wang, D.; Li, H.; Zheng, W. Oxidation behaviors of TA15 titanium alloy and TiBw reinforced TA15 matrix composites prepared by spark plasma sintering. *J. Mater. Sci. Technol.* **2019**, *37*, 46–54. [[CrossRef](#)]
14. Kumar, A.; Sapp, M.; Vincelli, J.; Gupta, M.C. A study on laser cleaning and pulsed gas tungsten arc welding of Ti–3Al–2.5V alloy tubes. *J. Mater. Process. Tech.* **2010**, *210*, 64–71. [[CrossRef](#)]

15. Lu, Y.; Ding, Y.; Wang, G.; Yang, L.; Wang, M.; Wang, Y.; Guo, B. Ultraviolet laser cleaning and surface characterization of AH36 steel for rust removal. *J. Laser Appl.* **2020**, *32*, 032023. [[CrossRef](#)]
16. Tian, Z.; Lei, Z.; Chen, X.; Chen, Y.; Zhang, L.-C.; Bi, J.; Liang, J. Nanosecond pulsed fiber laser cleaning of natural marine micro-biofoulings from the surface of aluminum alloy. *J. Clean. Prod.* **2020**, *244*, 118724. [[CrossRef](#)]
17. Tian, Z.; Lei, Z.; Chen, Y.; Chen, C.; Zhang, R.; Chen, X.; Bi, J.; Sun, H. Inhibition effectiveness of laser-cleaned nanostructured aluminum alloys to sulfate-reducing bacteria based on superwetting and ultraslippery surfaces. *ACS Appl. Bio Mater.* **2020**, *3*, 6131–6144. [[CrossRef](#)]
18. Shi, T.; Wang, C.; Mi, G.; Yan, F. A study of microstructure and mechanical properties of aluminum alloy using laser cleaning. *J. Manuf. Process.* **2019**, *42*, 60–66. [[CrossRef](#)]
19. Gao, Q.; Li, Y.; Wang, H.-E.; Liu, W.; Shen, H.; Zhan, X. Effect of scanning speed with UV laser cleaning on adhesive bonding tensile properties of CFRP. *Appl. Compos. Mater.* **2019**, *26*, 1087–1099. [[CrossRef](#)]
20. Zheng, B.; Jiang, G.; Wang, W.; Mei, X. Fabrication of superhydrophilic or superhydrophobic self-cleaning metal surfaces using picosecond laser pulses and chemical fluorination. *Radiat. Eff. Defects Solids* **2016**, *171*, 461–473. [[CrossRef](#)]
21. Zhuang, S.; Kainuma, S.; Yang, M.; Haraguchi, M.; Asano, T. Characterizing corrosion properties of carbon steel affected by high-power laser cleaning. *Constr. Build. Mater.* **2020**, *274*, 122085. [[CrossRef](#)]
22. Liu, B.; Mi, G.; Wang, C. Research on grain refinement and wear behavior of micro-remelted Ta15 alloy surface by laser cleaning. *Mater. Chem. Phys.* **2020**, *259*, 124022. [[CrossRef](#)]
23. Gong, Y.X.; Xu, J.; Buchanan, R.C. Surface roughness: A review of its measurement at micro-/nano-scale. *Phys. Sci. Rev.* **2018**, *3*, 1–10. [[CrossRef](#)]
24. Mieno, H.; Katsui, T. Experimental investigation of added frictional resistance by paint rough surface using a rotating cylinder. *J. Mar. Sci. Tech.* **2021**, *26*, 1–15. [[CrossRef](#)]
25. Wong, M.H.; Cheng, F.; Pang, G.; Man, H. Characterization of oxide film formed on NiTi by laser oxidation. *Mater. Sci. Eng. A* **2007**, *448*, 97–103. [[CrossRef](#)]
26. Liu, J.; Wu, G.; Li, S.; Yu, M.; Yi, J.; Wu, L. Surface analysis of chemical stripping titanium alloy oxide films. *J. Wuhan Univ. Technol. Sci. Ed.* **2012**, *27*, 399–404. [[CrossRef](#)]
27. Zhang, L.; Li, Y.; Guo, H.; Zhang, H.; Zhang, N.; Hayat, T.; Sun, Y. Decontamination of U(VI) on graphene oxide/Al₂O₃ composites investigated by XRD, FT-IR and XPS techniques. *Environ. Pollut.* **2019**, *248*, 332–338. [[CrossRef](#)]
28. McCafferty, E.; Wightman, J. An X-ray photoelectron spectroscopy sputter profile study of the native air-formed oxide film on titanium. *Appl. Surf. Sci.* **1999**, *143*, 92–100. [[CrossRef](#)]
29. Vasylyev, M.; Chenakin, S.; Yatsenko, L. Ultrasonic impact treatment induced oxidation of Ti6Al4V alloy. *Acta Mater.* **2016**, *103*, 761–774. [[CrossRef](#)]
30. Ouyang, P.; Mi, G.; Li, P.; He, L.; Cao, J.; Huang, X. Non-isothermal oxidation behavior and mechanism of a high temperature near- α titanium alloy. *Materials* **2018**, *11*, 2141. [[CrossRef](#)] [[PubMed](#)]